Ni /Fe_3O_4@Nanocellulose and Ni/Nanocellulose Green Nanocomposites: Inorganic- Organic Hybrid Catalysts for the Reduction of Organic Pollutants

Heidari, Hannaneh*[+]; Aliramezani, Fatemeh

Department of Inorganic Chemistry, Faculty of Chemistry, Alzahra University, Tehran, I.R. IRAN

ABSTRACT: *In this work, Ni NPs have been in-situ synthesized using hydrazine as a reducing agent and immobilized on nanofibrillated cellulose (Ni/NFC) and magnetic nanofibrillated cellulose (Ni/Fe_3O_4@NFC) as green supports. The structure and morphology of the Ni/Fe_3O_4@NFC nanocomposite clarified high purity single-phase spherical- shaped Ni nanoparticles of about 30 nm distributed on the surface of nanocellulose as compared to the larger size of star shape particle in Ni/NFC. The catalytic activity of both nanocomposites was investigated for the reduction of 4-nitrophenol (4-NP), Methyl Orange (MO), and Methylene Blue (MB). The results demonstrated high catalytic efficiency toward the removal of water pollutants in a short reaction time. The reduction rate constants (k) of freeze-dried Ni/Fe_3O_4@NFC catalyst were 30 ×10^{-3} s^{-1}, 17.3×10^{-3} s^{-1}, and 6.9 ×10^{-3} s^{-1}, for 4-NP, MO, and MB respectively, which were higher than those of synthesized Ni/NFC and other reported Ni-based catalysts. Moreover, the catalyst could be easily magnetically recoverable and reusable in other cycles.*

KEYWORDS: *Ni nanoparticle; Fe_3O_4; Catalytic activity; Nanocellulose.*

INTRODUCTION

Dyes such as 4-NP and MO are known common organic pollutants according to the Environmental Protection Agency (EPA). 4-NP belongs to the class of impurities, which is stable in the environment and resistant to biodegradation. Whereas 4-aminophenol (4-Ap), as reduced form of it, is a safety compound, less toxic, and it is regarded as a critical intermediate that can be used in many industries such as pharmaceutical, textile industries, photographic, and agrochemical. Methyl Orange (MO) as an azo dye is toxic, genotoxic, mutagenic, and has carcinogenic effects on aquatic living organisms [1, 2]. MB is a toxic cationic dye, which used in the textile industry. This dye may cause health problems [3].

Nanoscale magnetic metal crystals such as Fe, Co, Ni and Pd have attracted a lot of attention due to their unique properties, and diverse applications in various fields such as catalysts, Fuel cells, drug delivery, medical diagnosis, lithium-ion batteries, magnetic recording, solar cells, textile industry, optical filters, antibacterial activity and so on [4-12].

Fe_3O_4 NPs are very effective catalysts for the degradation of dye-containing water because of their excellent adsorption efficiency, surface reactivity,

** To whom correspondence should be addressed.*
+ E-mail: h.heidari@alzahra.ac.ir
1021-9986/2022/10/3293-3303 11/$/6.01

and large surface area. Previous reports showed that the degradation rate by adding another metal such as Ni, Cu, Co, Pd, Ag, and Pt with iron oxide nanoparticles might be improved, and prevents oxidation in the air [13-16]

Pure metallic nickel nanocrystals are synthesized using the sonochemical method, Chemical Vapor Deposition (CVD), microwave plasma deposition, ball milling, chemical/electrochemical methods, polyol process, spray-pyrolysis method, chemical reduction in the liquid phase, and many others. However, the preparation of nickel nano-structure materials is complex because they are easily oxidized. To overcome this problem, Ni nanoparticles have also been synthesized in the host matrix, such as Al_2O_3, activated carbon, Al-MCM 41, or in the polymer matrix [5, 17-20].

On the other hand, it is more effective to develop biocomposites as a renewable resource instead of synthetic polymer-based composites. Cellulose is an abundant, natural, and biodegradable biopolymer. It is created by repeating units of cellobiose. Nanocellulose is in the form of fibers or crystals having nano dimensions in length and high mechanical characteristics, and low density. Nanocellulose materials, through their unique properties, can be divided into three types: nanofibrillated cellulose (NFC), cellulose nanocrystals (CNC), and bacterial nanocellulose (BNC) [21, 22]. The unique morphology and reactive hydroxyl groups on the surface of nanocellulose make it suitable support for the synthesis of nanoparticles. The cellulosic nanocomposites have unique properties owing to the synergistic effect compared to nanomaterials alone. Nanocellulose also is a good stabilizer for metal nanoparticles, which can prevent aggregation and promote the homogeneous nucleation of nanoparticles [23]. Recently some groups have reported nanocellulose-based nanometal composites to degrade 4-NP, MO, and MB [24-30].

There are still some challenges in introducing a novel catalyst for removing toxic and non-biodegradable dyes from the environment. Therefore, this study aims to develop an effective method for removing organic pollutants from industrial-colored wastewater using a novel, green, and reusable magnetic catalyst based on nitrocellulose. Herein we report the in-situ synthesis of Ni nanoparticles with homogeneous distribution on the surface of different supports, including Fe_3O_4@NFC (Ni/Fe_3O_4 @NFC), and NFC (Ni/NFC) by hydrazine as a reducing agent. Then, the nanocomposites were characterized and further compared their catalytic activity to reduce three types of organic pollutants (4-NP, MO, and MB). Also, the reusability of Ni /Fe_3O_4 @NFC nanocatalyst was investigated.

EXPERIMENTAL SECTION

Materials and methods

Nanofibrillated cellulose (NFC) was purchased from a nanonovin polymer company, Iran. All other chemicals were purchased from Merck Company and were used without any further purification. The X-Ray Diffraction(XRD) patterns were recorded in a Rigaku Ultima IV X-ray diffractometer using Cu-Kα radiation at 40 kV and 30 mA. Fourier Transform InfraRed (FT-IR) spectroscopy spectra were collected on a Bruker Tensor 27 spectrometer using KBr disk. Field Emission Scanning Electron Microscopy (FE-SEM) was performed on a TESCAN MIRA3. The Energy Dispersive Spectroscopy (EDS) analysis was done using a SAMx-analyzer. ICP-OES vista-pro Varian-Inc. A UV-vis spectrophotometer was performed using Lambda-25 UV–Vis spectrometer (Perkin-Elmer, United States). TEM images have been taken with a Philips, model EM208S, instrument.

Synthesis of Fe_3O_4@NFC

The magnetic nanocellulose was prepared according to the previous report [33] as follows: 1.75 g $FeCl_3.6H_2O$ and 0.64 g $FeCl_2.4H_2O$ were added to 20 mL of nanofibrillated cellulose hydrogel (0.65 wt%) in 50 mL acetic acid solution (0.05 M) and stirred at 80 ℃. After 4 h, 2.88 mL of 25% NH_4OH was added dropwise into the reaction mixture under constant magnetic stirring for 30 min. Then, the product was easily separated by an external magnet, washed with distilled water and ethanol for several cycles, and dried at 60 ℃ in a vacuum oven.

Synthesis of Ni /Fe_3O_4 @NFC and Ni/NFC

For the preparation of Ni/Fe_3O_4@NFC nanocomposite, 1.78 g of $NiCl_2{\cdot}6H_2O$ was dissolved in 30 mL deionized water. Then 30 mL of $N_2H_4{\cdot}H_2O$ was added and stirred for 15 min (700 rpm). After that, the NaOH solution (2 M) was used to basify the pH to around 13. The obtained solution was added to 1 g Fe_3O_4@NFC and reflux at 100℃ under N_2 atmosphere until the black residue precipitated. After cooling to room temperature, the precipitate was separated

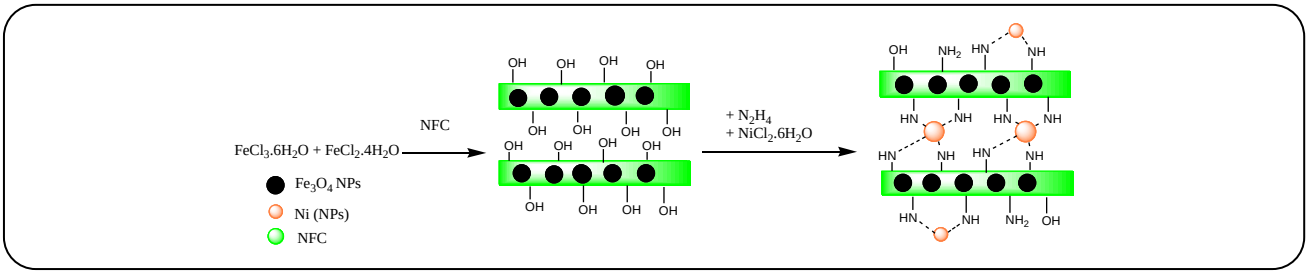

Scheme 1: Preparation of Ni/Fe$_3$O$_4$@NFC nanocatalyst

by a magnet and washed several cycles with ethanol and deionized water mixtures [31]. The product was dried using freeze-drying (-60 ℃, 16h). For comparison, Ni/NFC composite was also synthesized using 1.2 g of NFC hydrogel (0.65%) at 80 ℃ similar to the above procedure.

Catalytic Reduction of organic dyes

In a typical experiment, An aqueous suspension of 0.02 g of the dried composite was added into 0.25 mL of 20 mM aqueous solution containing dyes (4-NP or MO) (0.25 mL, 20 mM). Afterward, 0.25 mL of 5M freshly prepared sodium borohydride solution and 19.5 mL DI water were added under stirring at room temperature. Then, at appropriate time intervals, 0.5 mL of the reaction mixture filtered and the absorbance was recorded using a UV– vis spectrophotometer.

RESULTS AND DISCUSSION

Characterization

Fe_3O_4@NFC and NFC were used as supports and reducing agents for the synthesis of Ni NPs; however, no changes were observed on magnetic nanocellulose even after 24 h stirring under reflux conditions without an external reducing agent. So, using hydrazine hydrate as a reducing agent for the synthesis of Ni NPs is necessary (Scheme 1).

In the XRD pattern of prepared nickel nanoparticles (Fig. 1), three diffraction peaks at 2θ = 44.5°, 51.9°, and 76.6° corresponded to the (111), (200), and (220) crystallographic planes of the face-centered cubic (FCC) structure of metallic nickel (JCPDS No. 04-0850) [32]. Other weak diffraction peaks at 2θ values of 30, 35.3, 57.3, and 62.7 related to (220), (311), (511), and (440) planes could index to the FCC structure of Fe_3O_4 nanoparticles (JCPDS No.87-2334) [33]. The sharp peaks and lack of any impurities phases of NiO or $Ni(OH)_2$ showed the

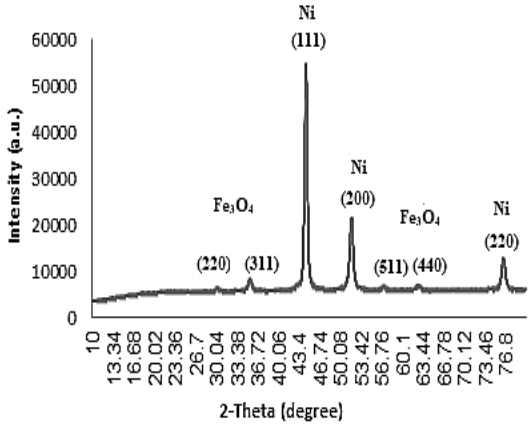

Fig. 1: XRD pattern of Ni/Fe$_3$O$_4$@NFC.

perfect phase purity, the excellent crystallinity character, and large particle size of Ni NPs.

The crystallite size (D) of Ni in the Ni/Fe_3O_4@NFC composite was also calculated using the Debye-Scherrer's formula (Eq. 1);

$$D = 0.9\lambda/(\beta \cos\theta) \quad (1)$$

Where, λ is the wavelength of the X-ray source (0.154 nm), β is the full width at half maximum intensity (FWHM) and θ is the angle of reflection measured in radians [34]. The (111) peak, the most intense for Ni in the composite, was used for the calculation of the crystallite size. The crystallite size was calculated to be 16 nm for Ni NPs in the Ni/Fe_3O_4@NFC composite.

FT-IR spectra of Fe_3O_4@NFC, Ni/ NFC, and Ni/Fe_3O_4@NFC were presented in Fig. 2. The absorption bands at 3446 cm^{-1} and 2925 cm^{-1} are attributed to the stretching vibrations of OH, and C–H bonds, respectively. In the Fe_3O_4@NFC, the peaks at 800 cm^{-1}, 577 cm^{-1}, and 466 cm^{-1} are related to the lattice vibration of tetrahedral and octahedral coordination compounds in the spinel structure of Fe–O groups [35-37]. The absorption bands

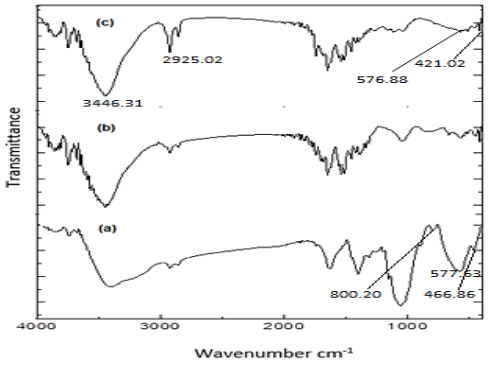

Fig. 2: FTIR spectra of a) Fe_3O_4@NFC, b) Ni/ NFC, c) Ni/Fe_3O_4@NFC.

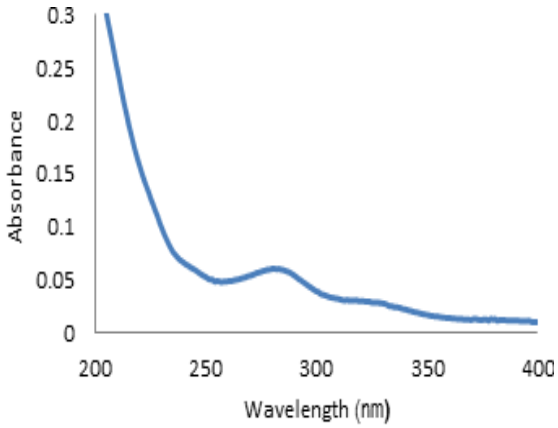

Fig. 3: UV–Vis adsorption spectrum of Ni/NFC nanocomposite.

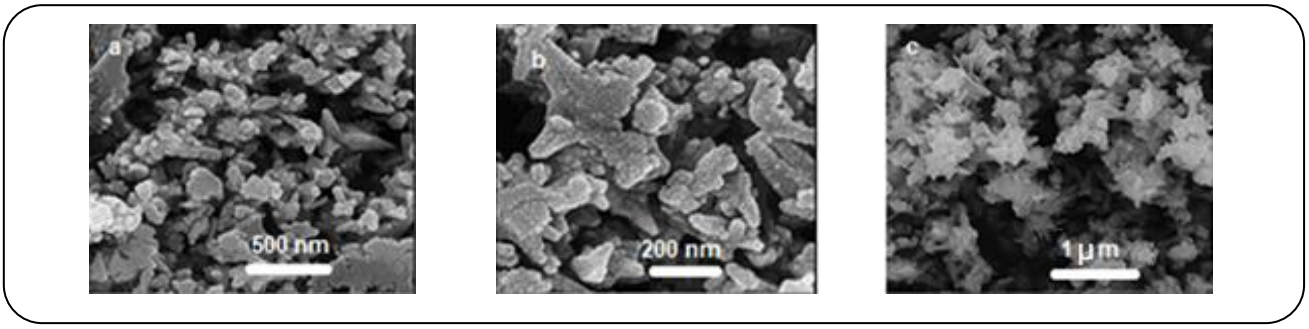

Fig. 4: FE-SEM micrographs of a, b) Ni/Fe_3O_4@NFC, and c) Ni/NFC.

at 421 cm^{-1} corresponding to the Ni-O stretching vibration modes [38].

UV–Vis spectrum of Ni NPs supported on NFC is shown in Fig. 3. The maximum absorption band at 280 nm is due to the formation of Ni nanoparticles. Li and Komarneni have reported that the Surface Plasmon Resonance (SPR) band at around 300 nm is related to Ni NPs [17].

The morphology of the as-prepared composites was investigated by the FE-SEM micrograph (Fig. 4). For Ni/Fe_3O_4@NFC nanocomposites, the clusters of spherical agglomerated nanoparticles were observed in the images (Fig. 4a, b). While Ni particles are star shapes in Ni/NFC nanocomposite (Fig. 4c).

More characterization to determine the elemental analysis and the immobilization of Ni species on the surface of the magnetic nanofibrillated cellulose also was carried out using EDX element color mapping measurements. The EDS analysis of Ni/Fe_3O_4@NFC nanocomposite confirmed that Fe and Ni elements deposited homogeneously on the surface of the nanocellulose. The Ni content in the Ni/Fe_3O_4@NFC nanocomposite catalyst as determined by ICP-OES analysis was 21.04 %.

As shown in Fig. 6. The TEM micrographs of the synthesized particles showed a typical core–shell structure with some agglomeration because of their magnetic nature. The dark internal core is found with a size range of about 30 nm and approximately spherical morphology in Ni/Fe_3O_4@NFC (Fig. 6a, b) While, in Ni/NFC (Fig. 6c, d) the star shape particles around 50-150 nm were observed which are comparable with FE-SEM results. The light external shell could be related to nitrocellulose.

The evaluation of the catalytic performance

The catalytic activity of the as-prepared nanocomposites was investigated in the reduction of 4-NP, MO, and MB with sodium borohydride ($NaBH_4$). According to the ratio of dye to reductant, an excessive amount of sodium borohydride was used in this reaction. Therefore, its concentration remains constant and the reaction occurs under pseudo-first-order conditions. The reduction of 4-NP, MO and MB spectrophotometrically followed at λ_{max} of 400 nm, 465 nm

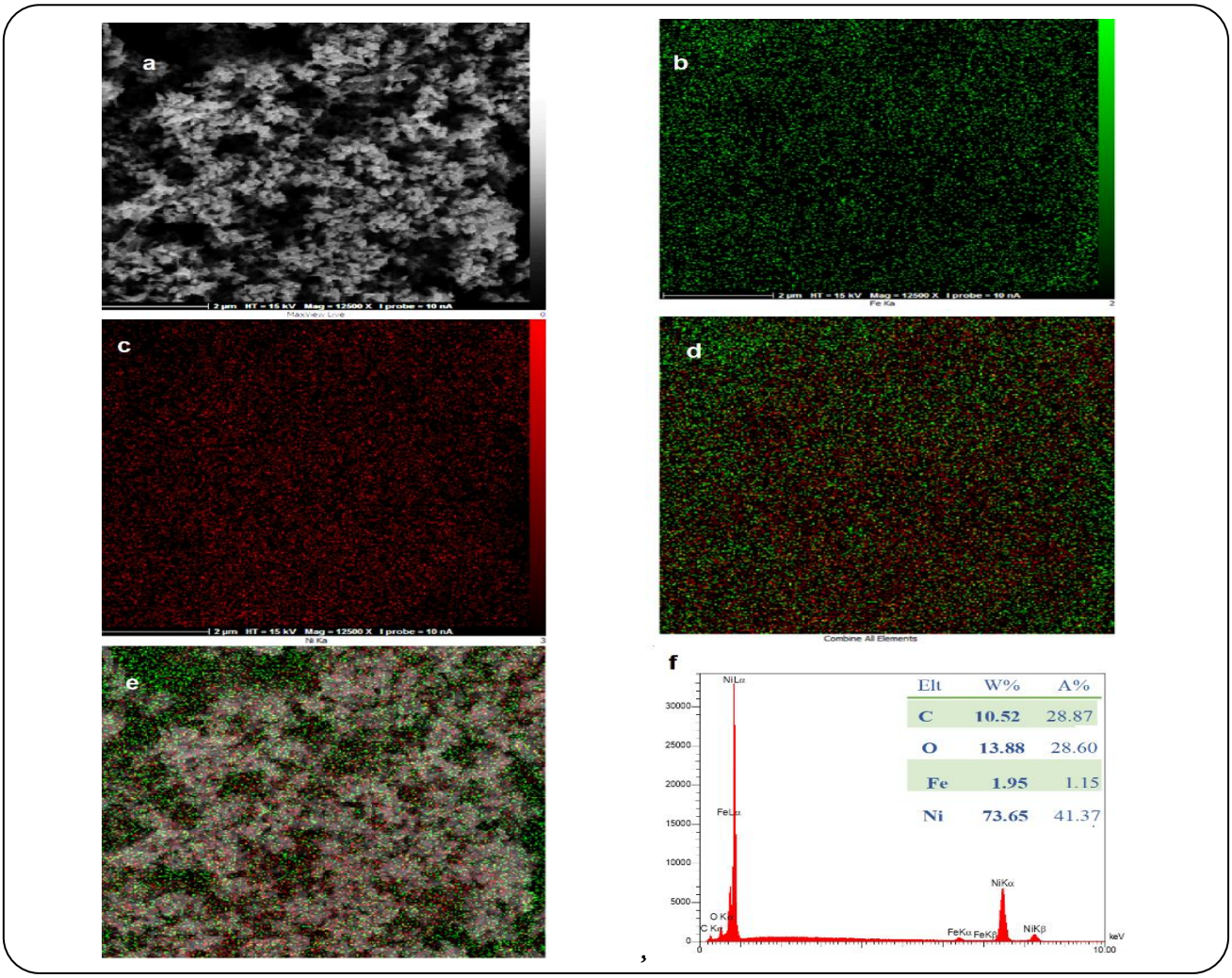

Fig. 5: EDX elemental mapping and spectrum of the Ni/Fe₃O₄@NFC nanocomposite.

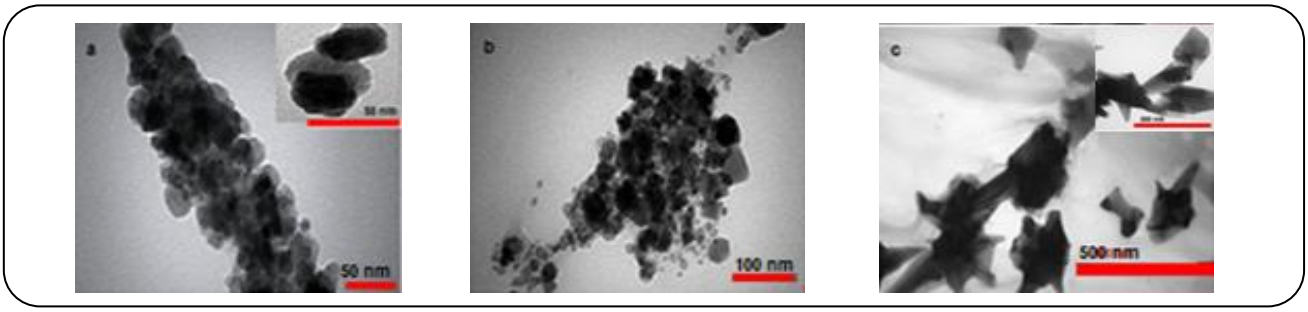

Fig. 6: TEM image of a, b) Ni/Fe₃O₄@NFC at different magnification (50 nm, 50 nm (inserted image), and 100 nm) and c) Ni/NFC nanocomposite at different magnification (500 nm and 200 nm (inserted image).

and 664 nm, respectively [33]. The plot of $\ln A_t$ versus time yielded a linear correlation for the Ni/Fe_3O_4@NFC as shown in Fig. 7. The pseudo-first-order rate constants (k) were calculated from Eq. (2) [39] to be 30×10^{-3}, 17.3×10^{-3} s^{-1} and 6.9×10^{-3} s^{-1} for the reduction of 4-NP, MO and MB, respectively.

$$\ln (A_t/A_0) = -kt \quad (1)$$

Where, A_t and A_0 are absorbance at time t and initial absorbance and k is the rate constant.

Furthermore, the calculated activity parameter values ($k' = k/m$), where m is the mass of the catalyst (g), and k is

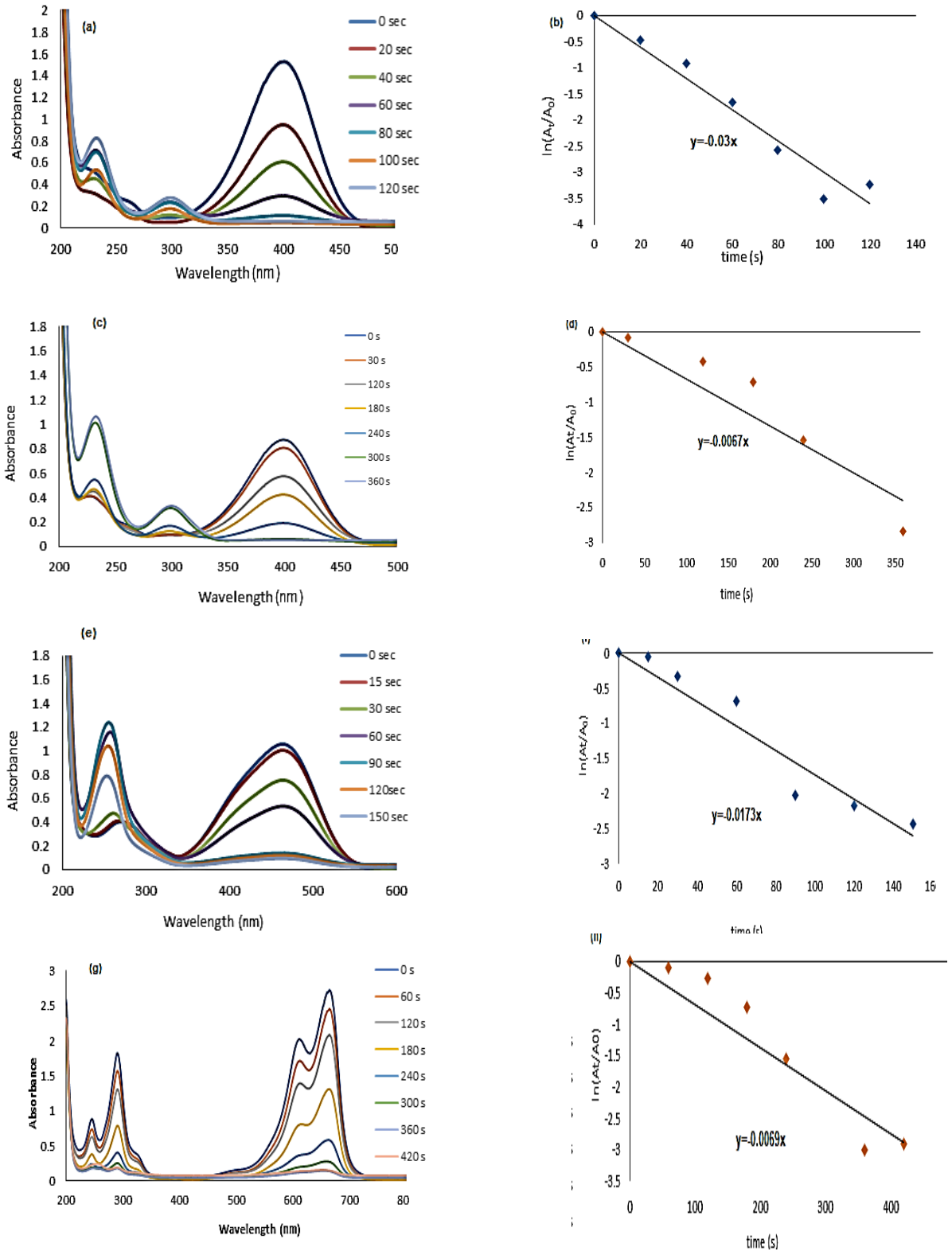

Fig. 7: UV–Vis spectra and the plot of Ln (A_t/A_0) versus time (a, b) freeze- dried and (c, d) air-dried Ni/Fe_3O_4@NFC catalyst. (e, f) UV–Vis spectra and the plot of Ln (A_t/A_0) versus time by Ni/Fe_3O_4@NFC freeze-dried catalyst for the reduction of MO, and (g, d) for the reduction of MB.

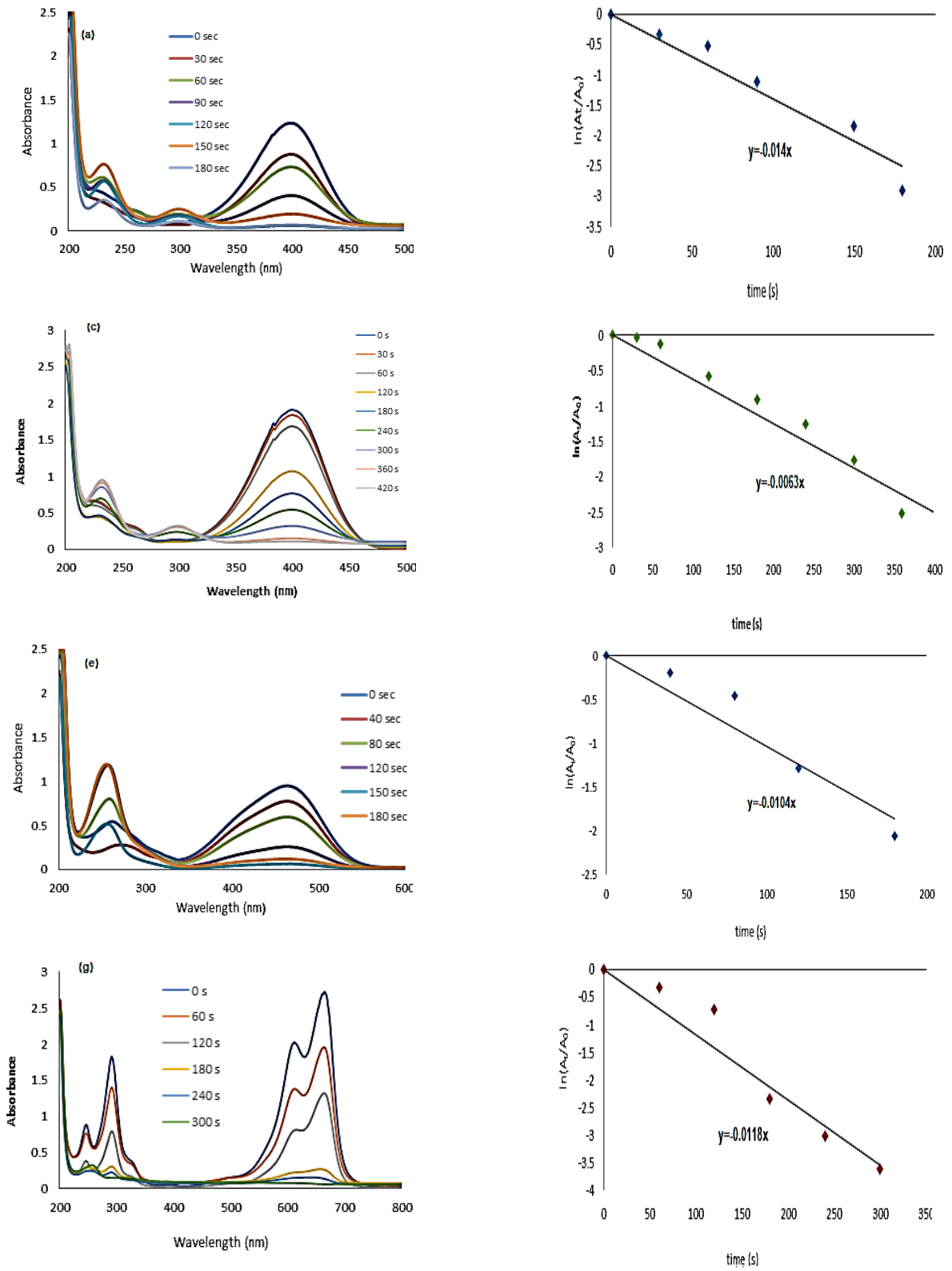

Fig. 8: UV–Vis spectra and the plot of Ln (A_t/A_0) versus time for the reduction of 4-NP by (a, b) freeze- dried and (c, d) air-dried Ni/ NFC catalyst. (e, f) UV–Vis spectra and the plot of Ln (A_t/A_0) versus time by Ni/ NFC freeze-dried catalyst for the reduction of MO, and (g, d) for the reduction of MB

Table 1: Comparison of catalytic performance of as-prepared Ni catalysts with other reported catalysts in reduction of 4-NP.

Entry	Catalyst	$C_{4\text{-NP}}$ (mM)	$k \times 10^{-3}$ (s^{-1})	Ref
1	Ni/CS-FP	100	1.93	[27]
2	Ni NPs/MCC	0.14	5.6	[28]
3	P(MAC)-Ni	10	12.5	[40]
4	Ni - RGO	0.1	1.8	[41]
5	Ni-Pd/NrGO	0.05	17	[42]
6	Ni/ NFC	20	14	This work
7	Ni/Fe_3O_4@NFC	20	30	This work

the apparent rate constant (s^{-1}) were determined 1.5, 0.86 and 0.34 s^{-1} g^{-1} for reduction of 4-NP, MO, and MB, respectively (Fig. 7). Whereas, the apparent rate constant (k and k′) of the Ni/NFC were calculated to be 14.0×10^{-3} s^{-1} and 0.7 s^{-1} g^{-1}, 10.4×10^{-3} s^{-1} and 0.52 s^{-1} g^{-1}, and 11.8×10^{-3} s^{-1} and o.59 s^{-1} g^{-1} for reduction of 4-NP, MO, and MB, respectively (Fig. 8). The results indicated that the Ni/Fe_3O_4@NFC nanocomposite had higher catalytic activity than the Ni/NFC. The enhanced catalytic activity of the Ni/Fe_3O_4@NFC could be attributed to the presence of both the Fe_3O_4 and the Ni nanoparticles with smaller particle size on the surface of nanocellulose and the effect of increased surface areas of composite. Moreover, it could be observed that the catalyst prepared by freeze-drying as compared to air-drying method demonstrated higher catalytic activity investigated in the previous report [33].

Considering previous literature [13], a plausible catalytic mechanism for the reduction of dye molecules has been suggested. In the reaction, BH_4^- as a nucleophile, transfers electrons to Ni/Fe_3O_4 nanoparticles and the dye molecule as the electrophile accepts the electrons leading to the reduced form. In this process, both nucleophile and electrophile are absorbed on the catalysts resulted in reduction of dyes.

The reusability of the catalyst was investigated repeatedly up to five cycles in 4-NP reduction. The nanocatalyst was magnetically separated after each run and washed with water for the next cycle under the same reaction conditions. As can be seen, the catalytic efficiency [39] decreased gradually which may be due to the loss of catalyst after each catalytic run and the decomposition of the surface intermediates (Fig. 9).

The catalytic activity of the present Ni/Fe_3O_4@NFC catalyst was compared with the other reported Ni catalysts (Table 1), which indicates the higher catalytic activity of the synthesized catalyst for the degradation of 4-NP.

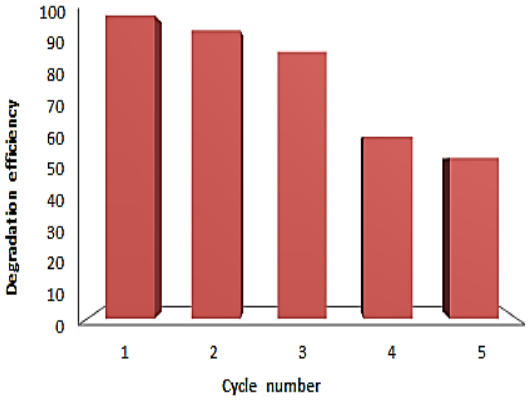

Fig. 9: Reusability of for the degradation of 4-NP. All experiments for catalyst reuse were performed for 60 s

CONCLUSIONS

In summary, synthesis of novel Ni/Fe_3O_4@NFC and Ni/NFC composites using the simple method by nanofibrillated cellulose as inexpensive and green support resulted in spherical and star-shaped particles. The new Ni/Fe_3O_4@NFC magnetic nanocomposite showed the best catalytic activity to remove hazardous substances (4-NP, MO, and MB) under mild reaction conditions as compared to other reports. The catalyst also could be easily magnetically separated and reused for other cycles.

Acknowledgements

The Authors gratefully acknowledge from the Research Council of Alzahra University for financial support.

Received : Jul. 27, 2021 ; Accepted : Nov. 29, 2021

REFERENCES

[1] Ahsan M.A., Fernandez-Delgado O., Deemer E., Wang H., El-Gendy A., Curry M., Noveron J., Carbonization of Co-BDC MOF Results in Magnetic C@Co Nanoparticles that Catalyze The Reduction of Methyl Orange and 4-Nitrophenol in Water, *J. Mo.l Liq.*, **290**: 111059 (2019).

[2] Gupta N.K., Ghaffari Y., Kim S., Bae J., Kim K.S., Saifuddin M., Photocatalytic Degradation of Organic Pollutants over MFe_2O_4 (M = Co, Ni, Cu, Zn) Nanoparticles at Neutral pH, *Sci Rep.*, **10**: 4942 (2020).

[3] Ghosh I., Kar S., Chatterjee T., Bar N., Das S K., Removal of Methylene Blue from Aqueous Solution Using Lathyrus sativus husk: Adsorption Study, MPR and ANN Modelling, *Process Saf. Environ. Prot.*, **149**: 345-361(2021).

[4] Schrittwieser S., Reichinger D., Schotter J., Applications, Surface Modification and Functionalization of Nickel Nanorods, *Materials*., **11**: 45 (2017).

[5] Foo Y.T., Chan J.E.M., Ngoh G.C., Abdullah A., Horri B., Salamatinia B., Synthesis and Characterization of NiO and Ni Nanoparticles Using Nanocrystalline Cellulose (NCC) as a Template, *Ceram Int*., **43**:16331-16339 (2017).

[6] Fekri M.H., Tousi F., Heydari R., Razavi Mehr M., Rashidipour M., Synthesis of Magnetic Novel Hybrid Nanocomposite (Fe_3O_4@SiO_2/Activated carbon (by a Green Method and Evaluation of Its Antibacterial Potential, *Iranian Journal of Chemistry and Chemical Engineering (IJCCE)*, **41(3)**: 767-776 **(**2021**)**.

[7] Goodarzi M., Joukar S., Ghanbari D., Hedayati K., $CaFe_2O_4$–ZnO Magnetic Nanostructures: Photo Degradation of Toxic Azo-Dyes Under UV irradiation, *J Mater Sci: Mater Electron*, **28**: 12823–12838 (2017).

[8] Hedayati K., Azarakhsh S., Saffari J., Ghanbari D., Magnetic and Photo-catalyst $CoFe_2O_4$-CdS Nanocomposites: Simple Preparation of Ni, Co, Zn or Ag-Doped CdS Nanoparticles, *J. Mater. Sci: Mater. Electron*, **28**: 5472–5484 (2017).

[9] Lahijani B., Hedayati K., Goodarzi M., Magnetic $PbFe_{12}O_{19}$-TiO_2 Nanocomposites and their Photocatalytic Performance in the Removal of Toxic Pollutants, *Main Group Metal Chemistry*, **41**: 53–62 (2018).

[10] Song Q., Wang W.D., Lu K., Li F., Wang B., Sun L., Ma J., Zhu H., Li B., Dong Z., Three-Dimensional Hydrophobic Porous Organic Polymers Confined Pd Nanoclusters for Phase-Transfer Catalytic Hydrogenation of Nitroarenes In Water, *Chem. Eng. J*, **415**: 128856 (2021).

[11] Zhu Y., Wang W.D., Sun X., Fan M., Hu X., Dong Z., Palladium Nanoclusters Confined in MOF@COP as a Novel Nanoreactor for Catalytic Hydrogenation, *ACS Appl. Mater. Interf.*, **12(6)**: 7285-7294, (2020).

[12] Zhu Y., Wang W.D., Sun X., Fan M., Hu X., Dong Z., Palladium Clusters Confined in Triazinyl-Functionalized COFs with Enhanced Catalytic Activity, *Appl. Catal. B: Environ*, **257**: 117942 (2019).

[13] Prasad C., Sreenivasulu K., Gangadhara S., Venkateswarlu P., Bio Inspired Green Synthesis of Ni/Fe_3O_4 Magnetic Nanoparticles Using Moringa Oleifera Leaves Extract: A Magnetically Recoverable Catalyst for Organic Dye Degradation in Aqueous Solution, *J. Alloys Compd.*, **700**: 252-258 (2017).

[14] Liu W-J., Qian T-T., Jiang H., Bimetallic Fe Nanoparticles: Recent Advances in Synthesis and Application in Catalytic Elimination of Environmental Pollutants, *Chem. Eng. J.*, **236**: 448-463 (2014).

[15] Baye A.F., Appiah-Ntiamoah R., Kim H., Synergism of Transition Metal (Co, Ni, Fe, Mn) Nanoparticles and "Active Support" Fe_3O_4@C for Catalytic Reduction of 4-nitrophenol, *Sci. Total. Environ*, **712**:135492 (2020)

[16] Mardani H.R., (Cu/Ni)–Al Layered Double Hydroxides@Fe3O4 as Efficient Magnetic Nanocomposite Photocatalyst for Visible-Light Degradation of Methylene Blue, *Res. Chem. Intermed.*, **43**: 5795-5810 (2017).

[17] Li D., Komarneni S., Microwave-Assisted Polyol Process for Synthesis of Ni Nanoparticles, *J. Am. Ceram. Soc.*, **89**:1510 (2006).

[18] Wu Z.G., Munoz, M., Montero O., The Synthesis of Nickel Nanoparticles by Hydrazine Reduction, *Adv. Powder Technol*., **21**:165-168 (2010).

[19] Thiruvengadam V., Vitta S., Ni–Bacterial Cellulose Nanocomposite; A Magnetically Active Inorganic–Organic Hybrid Gel, *RSC Advances*., **3**: 12765-12773 (2013).

[20] Wu Z., He X., Gao Z., Xue Y., Chen X., Zhanget L., Synthesis and Characterization of Ni-Doped Anatase TiO2 Loaded in Magnetic Activated Carbon for Rapidly Removing Triphenylmethane Dyes, *Environ. Sci. Pollut. Res.*, **28**: 3475-3483 (2021).

[21] Sharma A., Thakur M., Bhattacharya M., Mandal T., Goswami S., Commercial Application of Cellulose Nano-Composites – A Review, *Biotechnol Reports*., **21**:e00316 (2019).

[22] Teo H.L., Wahab R.A., Towards an Eco-Friendly Deconstruction of Agro-Industrial Biomass and Preparation of Renewable Cellulose Nanomaterials: A Review, *Int. J. Biol. Macromol*., **161:**1414-1430 (2020).

[23] Zhang Q., Zhang L., Wu W., Xiao H., Methods and Applications of Nanocellulose Loaded with Inorganic Nanomaterials: A Review, *Carbohydr. Polym.*, **229**: 115454 (2020).

[24] Eisa W.H., Abdelgawad A.M., Rojas, O.J., Solid-State Synthesis of Metal Nanoparticles Supported on Cellulose Nanocrystals and Their Catalytic Activity, *ACS Sustain Chem. Eng*., **6**:3974-3983 (2018).

[25] Esquivel-Pena V., Guccini V., Kumar S., Salazar-Alvarez G., Rodrıguez, E., Gyves, J., Hybrids Based on Borate-Functionalized Cellulose Nanofibers and Noble-Metal Nanoparticles as Sustainable Catalysts For Environmental Applications, *RSC Adv*., **10**: 12460-12468 (2020)

[26] An X., Long Y., Ni Y., Cellulose Nanocrystal/ Hexadecyltrimethylammonium Bromide/Silver Nanoparticle Composite as a Catalyst for Reduction of 4-nitrophenol, *Carbohydr Polym*., **156**: 253-258 (2016).

[27] Yang Y., Chen Z., Wu X., Zhang X., Nanoporous Cellulose Membrane Doped with Silverfor Continuous Catalytic Decolorization of Organic Dyes, *Cellulose*., **25**: 2547-2558 (2018).

[28] Kamal T., Khan S.B., Asiri A.M., Nickel nanoparticles-Chitosan Composite Coated Cellulose Filter Paper: An Efficient and Easily Recoverable Dip-Catalyst for Pollutants Degradation, *Environ Pollut*., **218**: 625-633 (2016)

[29] Yu Y., Liu S., Pei Y., Luo X., Growing Pd NPs on Cellulose Microspheres *via* in-Situ Reduction for Catalytic Decolorization of Methylene Blue, *Int. J. Biol. Macromol*., **166**:1419-1428 (2021).

[30] Su X., Chen W., Han Y., Wang D., Yao J., In-Situ Synthesis of Cu2O on Cotton Fibers with Antibacterial Properties and Reusable Photocatalytic Degradation of Dyes, *Appl. Surf. Sci*., **536**:147945 (2021)

[31] Zeynizadeh B., Karami S., Synthesis of Ni Nanoparticles Anchored on Cellulose Using Different Reducing Agents and their Applications Towards Reduction of 4-Nitrophenol, *Polyhedron*., **166**: 196-202 (2019).

[32] Wang F., Zhao D., Zhang L., Fan L., Zhang X., Hu S., Nanostructured Nickel Nitride with Reduced Graphene Oxide Composite Bifunctional Electrocatalysts for an Efficient Water-Urea Splitting, *Nanomaterials*., **9**: 1583 (2019).

[33] Heidari H., Aliramezani F., Reductant-Free and In-Situ Green Synthesis of Ag Nanoparticles on Fe_3O_4@Nanocellulose and Their Catalytic Activity for the Reduction of Dyes, *Chemistry Select*., **6**: 1223-1229 (2021).

[34] Abbasi L., Hedayati K., Ghanbari D., Magnetic Properties and Kinetic Roughening Study of Prepared Polyaniline: Lead Ferrite, Cobalt Ferrite and Nickel Ferrite Nanocomposites Electrodeposited Thin Films, *J. Mater. Sci.: Mater. Electron*., **32**: 14477–1449 (2021).

[35] Sivakumar P., Ramesh R., Ramanand A., Ponnusamy S., Muthamizhchelvan C., Synthesis and Characterization of Nickel Ferrite Magnetic Nanoparticles, *Mater. Res. Bull*., **46**: 2208-2211 (2011).

[36] Laokul P., Amornkitbamrung V., Seraphin S., Maensiri S., Characterization and Magnetic Properties of Nanocrystalline $CuFe_2O_4$, $NiFe_2O_4$, $ZnFe_2O_4$ Powders Prepared by the Aloe Vera Extract Solution, *Curr Appl Phys.*, **11**:101-108 (2011).

[37] Elmoussaoui, H., Hamedoun, M., Mounkachi, O., Benyoussef, A., Masrour, R., Hlil, E., New Results on Magnetic Properties of Tin-Ferrite Nanoparticles, *J. Supercond Nov. Magn*., **25**:1995-2002 (2012)

[38] Kashani Motlagh M.M., Youzbashi A.A., Hashemzadeh F., Sabaghzadeh L., Structural Properties of Nickel Hydroxide/Oxyhydroxide and Oxide Nanoparticles Obtained by Microwave-Assisted Oxidation Technique, *Powder Technol.*, **237**:562-568 (2013).

[39] Heidari, H., Karbalaee, M., Ultrasonic Assisted Synthesis of Nanocrystalline Cellulose as Support and Reducing Agent for Ag Nanoparticles: Green Synthesis and Novel Effective Nanocatalyst for Degradation of Organic Dyes, *Appl. Organomet. Chem.*, **33(9)**:e5070 (2019)

[40] Ajmal, M., Siddiq, M., Al-Lohedan, H., Sahiner, N., Highly Versatile p(MAc)-M (M:Cu, Co, Ni) Microgels Composite Catalyst for Individual and Simultaneous Catalytic Reduction of Nitro Compounds and Dyes, *RSC Adv.*, **4**:59562-59570 (2014)

[41] Tian Y., Liu Y., Pang F., Wang F., Zhang X., Green Synthesis of Nanostructed Ni-Reduced Graphene Oxide Hybrids and their Application for Catalytic Reduction of 4-Nitrophenol, *Colloids Surfaces A Physicochem Eng Asp*., **464**: 96-103 (2015).

[42] Liu L., Chen R., Liu W., Wu J., Gao D., Catalytic Reduction of 4-nitrophenol over Ni-Pd Nanodimers Supported on Nitrogen-Doped Reduced Graphene Oxide, *J. Hazard. Mater*., **320**: 96-104 (2016).